Nuclear Instruments and Methods in Physics Research B 359 (2015) 36–43

Contents lists available at ScienceDirect

Nuclear Instruments and Methods in Physics Research B

journal homepage: www.elsevier.com/locate/nimb

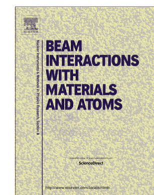

Temperature effect on betavoltaic microbatteries based on Si and GaAs under ^{63}Ni and ^{147}Pm irradiation

Hao Wang [a], Xiao-bin Tang [a,b,*], Yun-Peng Liu [a], Zhi-Heng Xu [a], Min Liu [a], Da Chen [a,b]

[a] *Department of Nuclear Science and Engineering, Nanjing University of Aeronautics and Astronautics, Nanjing, China*
[b] *Jiangsu Key Laboratory of Material and Technology for Energy Conversion, Nanjing, China*

ARTICLE INFO

Article history:
Received 30 May 2015
Received in revised form 10 July 2015
Accepted 13 July 2015

Keywords:
Betavoltaic microbatteries
Temperature effects
Energy conversion devices
Beta sources

ABSTRACT

The effect of temperature on the output performance of four different types of betavoltaic microbatteries was investigated experimental and theoretical. Si and GaAs were selected as the energy conversion devices in four types of betavoltaic microbatteries, and ^{63}Ni and ^{147}Pm were used as beta sources. Current density–voltage curves were determined at a temperature range of 213.15–333.15 K. A simplified method was used to calculate the theoretical parameters of the betavoltaic microbatteries considering the energy loss of beta particles for self-absorption of radioactive source, the electron backscatter effect of different types of semiconductor materials, and the absorption of dead layer. Both the experimental and theoretical results show that the short-circuit current density increases slightly and the open-circuit voltage (V_{OC}) decreases evidently with the increase in temperature. Different combinations of energy conversion devices and beta sources cause different effects of temperature on the microbatteries. In the approximately linear range, the V_{OC} sensitivities caused by temperature for ^{63}Ni–Si, ^{63}Ni–GaAs, ^{147}Pm–Si, and ^{147}Pm–GaAs betavoltaic microbatteries were −2.57, −5.30, −2.53, and −4.90 mV/K respectively. Both theoretical and experimental energy conversion efficiency decreased evidently with the increase in temperature.

© 2015 Elsevier B.V. All rights reserved.

1. Introduction

In recent years, microelectromechanical systems (MEMS) have played an important role in the rapid development of military, aerospace, biomedical, industrial, and agricultural fields [1]. As an important part of MEMS, micropower is one of the bottlenecks that affect its development. Thus micropower has attracted considerable research attention [2]. A betavoltaic microbattery has potential long life, high energy density, stability, miniaturization, no external power supply, which make it compact and light, with small footprint. These characteristics are modified with the development of micropower [3–5]. In 2002, Blanchard's research team demonstrated that the energy released from a radioactive element could serve as a power source of a MEMS [6]. With the development of semiconductors, MEMS, based on the power supply for betavoltaic microbatteries, has broad application prospects in polar sea, desert, and space exploration. Temperatures in these environments significantly vary. Daytime temperatures in the desert can reach up to 50 °C, whereas Antarctic temperature reaches as low as −90 °C. In addition, daytime temperatures on the lunar surface can reach as high as 127 °C as low as −183 °C at night. Therefore, temperature dependence is an important issue.

The effects of temperature on betavoltaic microbatteries has been investigated. Wang [7], Liu [8], and Nejad [9] studied ^{63}Ni–Si betavoltaic microbatteries. Chandrashekhar [10] analyzed ^{63}Ni–4H–SiC betavoltaic microbatteries. These studies indicate that the short-circuit current density (J_{SC}) slightly increases, whereas the open-circuit (V_{OC}) decreases significantly with the increase in temperature. These studies focused on the single-beta source and the single-energy conversion device. For practical applications, the effects of temperature on more kinds of betavoltaic microbatteries should be studied.

In the current paper, ^{63}Ni and ^{147}Pm sources are chosen as the two types of beta sources, and Si and GaAs are selected as the two energy conversion devices. Hence, four types of betavoltaic microbatteries are fabricated. The effects of temperature on the characteristic parameters of the betavoltaic microbatteries are studied in a temperature ranging from 213.15 to 333.15 K. The energy loss of beta particles for self-absorption of the radioactive source, the influence of electron backscattering from different semiconductor materials, and the absorption of the dead layer

* Corresponding author at: Department of Nuclear Science and Engineering, Nanjing University of Aeronautics and Astronautics, Nanjing, China. Tel.: +86 13601582233; fax: +86 025 52112906 80407.
E-mail address: tangxiaobin@nuaa.edu.cn (X.-b. Tang).

http://dx.doi.org/10.1016/j.nimb.2015.07.046
0168-583X/© 2015 Elsevier B.V. All rights reserved.

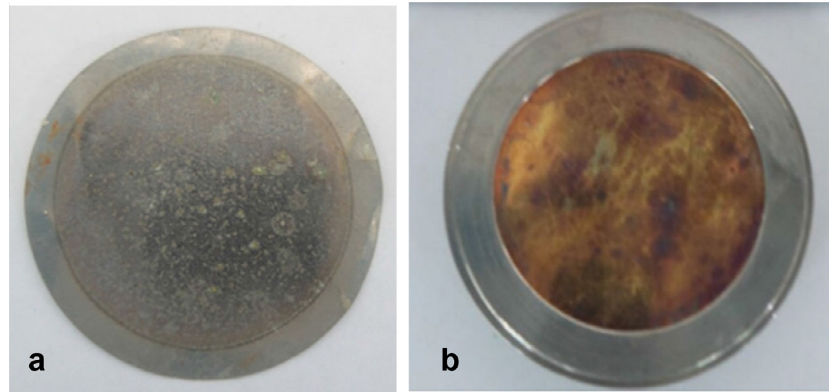

Fig. 1. Radioactive sources used in the experiment: (a) ^{63}Ni and (b) ^{147}Pm.

Table 1
Basic parameters of the radioactive sources.

Isotopes	Active area diameter (mm)	Factory apparent activity density (mCi/cm^2)	Apparent activity density in testing (mCi/cm^2)	Maximum energy (keV)	Average energy (keV)
^{63}Ni	25	5	4.889	65.87	20.532
^{147}Pm	25	5	2.130	224.7	62.576

are considered in the investigation. The characteristic parameters include J_{SC}, reverse saturation current density and V_{OC}.

2. Materials and methods

2.1. Radioactive sources and energy conversion devices

Betavoltaic microbatteries are primarily composed of radioactive sources and energy conversion devices. For convenience, the betavoltaic microbatteries that are based on Si and under the irradiation of ^{63}Ni are named ^{63}Ni–Si, the three other microbatteries are ^{147}Pm–Si, ^{63}Ni–GaAs, and ^{147}Pm–GaAs. Fig. 1 shows the radioactive sources used in experiment. The basic parameters are listed in Table 1. Based on the factory apparent activity density, apparent activity density in testing was calculated using the law of radioactive source decay. The average energy of the beta particles emitted from radioactive sources can be calculated by Monte Carlo particle transport code [11,12].

Given that the semiconductor materials have different bandgaps, Si and GaAs were prepared using an early maturation process technology, which has relatively low production cost among the current manufacturing processes. These materials are widely used in solar cells, MEMS, and other devices, as well as in many studies on isotope microbatteries [7,9,13]. Fig. 2 shows the energy conversion devices, structural representation and their basic parameters are listed in Table 2. The thickness of the dead layer (w_{d1}) is the thickness of the heavily doped region on the surface of energy conversion devices.

2.2. Experiment and measurement

The high and low temperature–humidity test chamber (Model 641A, DRK, CHINA) was used to control the temperature in the test environment. All the four types of betavoltaic microbatteries, namely, ^{63}Ni–Si, ^{147}Pm–Si, ^{63}Ni–GaAs, and ^{147}Pm–GaAs, were evaluated. At the temperature of 213.15–333.15 K, the current density–voltage (J–V) curves of the betavoltaic microbatteries were tested every 10 K by using a dual-channel system sourcemeter (Model 2636A, Keithley, USA). Fig. 3 shows the entire testing system, in which the ^{147}Pm–Si betavoltaic microbattery was being tested.

2.3. Theoretical analysis

For betavoltaic microbatteries, beta particles emitted from the radioactive source pass through a dead layer of semiconductor material into the p–n junction and generate electron–hole pairs by ionization and excitation. Electron–hole pairs move to the ends of the junction under the action of an electric field and generate current if the microbatteries are connected with an external resistor.

In this article, the energy loss of beta particles for the self-absorption of a radioactive source, the electron backscatter effect of different semiconductor materials, and the absorption of dead layer are considered. Supposing that all electron–hole pairs are recombined in the dead layer and the collection efficiency is 0% and that all the electron–hole pairs are collected outside the dead layer, and the collection efficiency is 100%, J_{SC} can be determined by [14]:

$$J_{SC} = \frac{q}{\varepsilon} E_\alpha A_\alpha (1-\eta_\beta)\exp(-\mu w_{d1})(1-\exp(-\mu w_{d2})), \quad (1)$$

where q is the electric charge in coulombs, ε is the energy required for the formation of an electron–hole pair, E_α is the average energy of beta particles emitted from the radioactive source surface after the self-absorption, A_α is the surface activity density of the radioactive source, η_β is the electron backscatter coefficient, μ is the linear attenuation coefficient, w_{d1} is the thickness of the dead layer, and w_{d2} is the thickness of the semiconductor intrinsic layer. In addition, ε can be computed by [15]:

$$\varepsilon = 2.8E_g + 0.5, \quad (2)$$

where E_g is the bandgap of the semiconductor material. E_g is related to temperature and can be expressed by [16]:

$$E_g(T) = E_g(0) - \frac{\alpha T^2}{T+\beta}, \quad (3)$$

where $E_g(0)$ is the bandgap when the temperature is 0 °C, α and β are constants related to the materials. For Si, the $E_g(0)$, α, and β

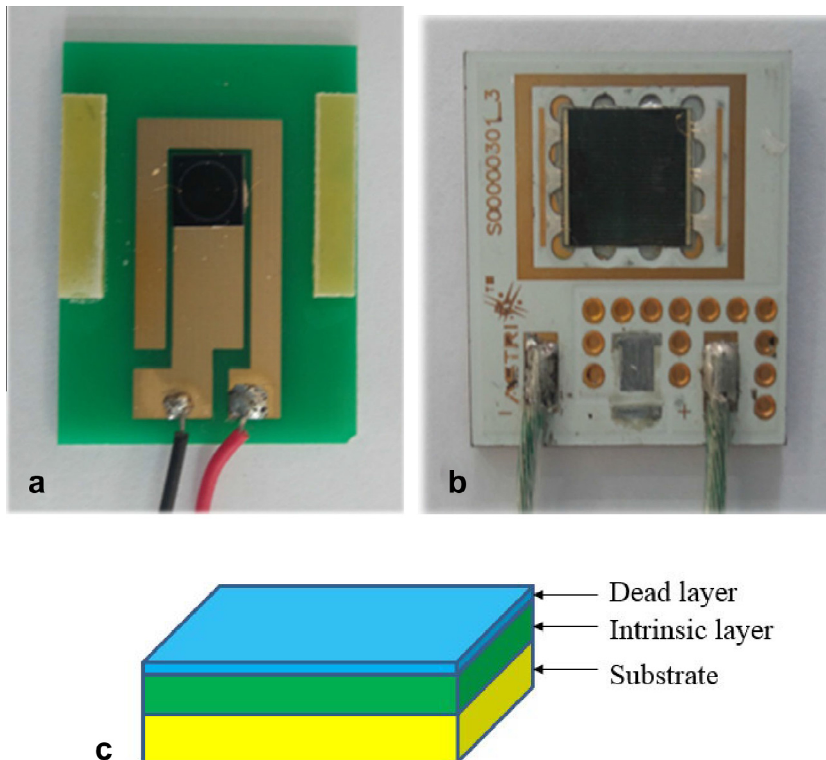

Fig. 2. Two kinds of energy conversion devices used in experiment: (a) Si and (b) GaAs; (c) the structural representation of energy conversion device.

Table 2
Basic parameters of the two kinds of energy conversion devices.

Material	Type of substrate impurity	Substrate doping concentration (cm^3)	Substrate thickness (μm)	Sensitive area (cm^2)	Intrinsic layer (μm)	Dead-layer thickness (μm)
GaAs	N	1–4 × 1018	350	1	4	0.53
Si	P	9.3 × 1013	300	0.25	300	0.68

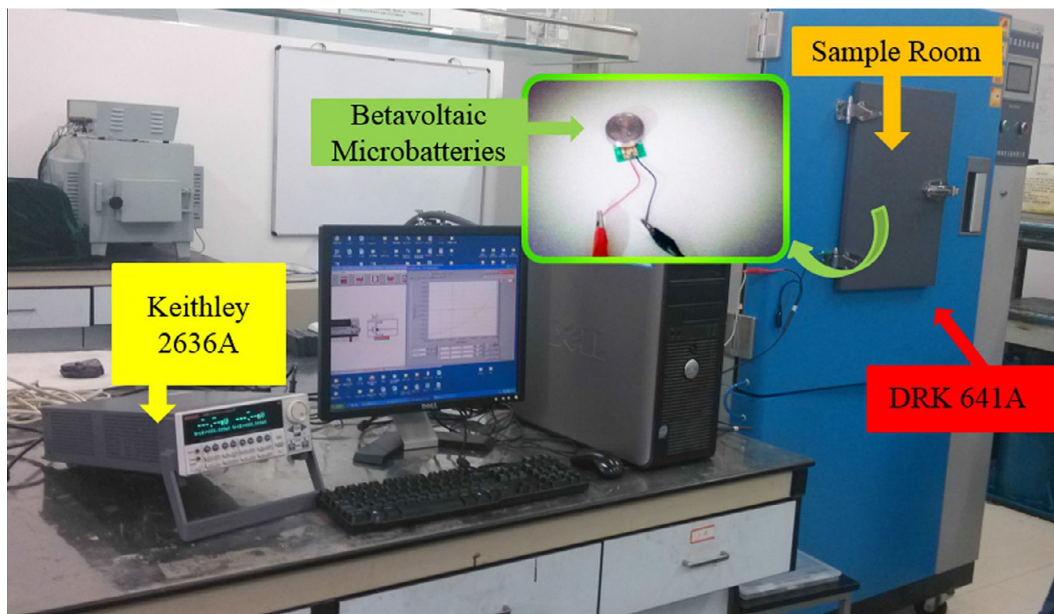

Fig. 3. Testing system for the effect of temperature on betavoltaic microbatteries.

Table 3
Values of μ of the betavoltaic microbatteries.

Betavoltaic microbattery	μ (cm^{-1})
^{63}Ni–Si	1037.024
^{63}Ni–GaAs	1212.519
^{147}Pm–Si	167.652
^{147}Pm–GaAs	196.024

Table 4
The η_β of Si and Ge irradiated by ^{63}Ni and ^{147}Pm.

Material	η_β	
	For the energy of 20.532 keV	For the energy of 62.576 keV
Si	0.169	0.149
Ge	0.327	0.319

values are 1.17 eV, 4.73×10^{-4} eV/K, and 636 K, respectively. For GaAs, the $E_g(0)$, α, and β values are 1.519 eV, 5.405×10^{-4} eV/K, and 204 K, respectively. For ^{63}Ni and ^{147}Pm, the E_α values are 20.532 and 62.576 keV respectively [11]. μ can be determined using [17]:

$$\mu = 15.2 \frac{Z^{4/3}}{A} \frac{1}{E_{max}^{1.485}}, \tag{4}$$

where Z, A, and E_{max} are the relative atomic number, relative atomic mass, and the maximum energy in the β energy spectrum, respectively. According to ICRP 38 [18], the E_{max} of ^{63}Ni and ^{147}Pm are 6.587×10^{-2} and 2.247×10^{-1} MeV, respectively. The μ of the four types of betavoltaic microbatteries are listed in Table 3.

When the beta beam irradiates the sample, the electrons diffract within the sample, change direction, and are likely to lose part of the energy. In the elastic scattering and inelastic scattering processes, the accumulated scattering angle of the incident electrons exceeds 90°. These electrons become backscattered electrons and escape from the surface of the sample. According to Drescher H et al. [19], the electron backscatter coefficient (η_β) is related to the atomic number of the material and the energy of the incident particle. Irradiated by ^{63}Ni and ^{147}Pm, the η_β of Si and GaAs are listed in Table 4. The η_β of GaAs cannot be obtained directly. Given that the atomic numbers of Ga and As are very close (31 and 33 respectively), the η_β of Ge with an atomic number of 32 is used to replace that of GaAs.

Thus, J_{SC} of the betavoltaic microbatteries can be calculated using Eq. (1). When energy conversion devices have ideal p–n junctions, V_{OC} of betavoltaic microbatteries can be expressed as:

$$V_{oc} = \frac{nkT}{q} \ln\left(\frac{J_{sc}}{J_0} + 1\right), \tag{5}$$

where n, k, T, and J_0 are the ideality factor, Boltzmann's constant, the temperature (in K), and J_0 respectively. In theoretical calculation, the n values for Si and GaAs are equal to 1 and 2, respectively.

3. Results and discussion

3.1. Measurement of J–V curves

The J–V curves of the four types of betavoltaic microbatteries were measured at a temperature range of 213.15–333.15 K. The results are shown in Fig 4. The trends of all of the J–V curves are

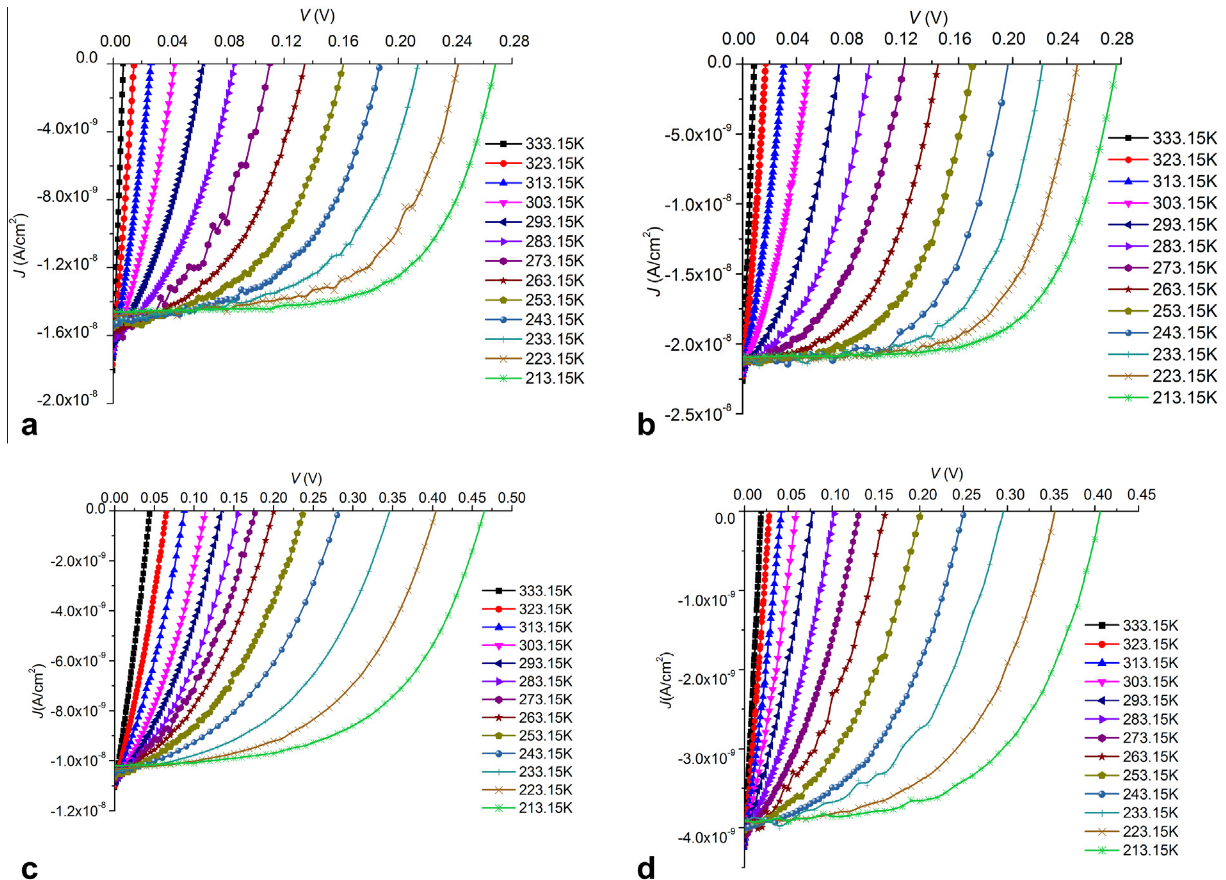

Fig. 4. The J–V curves of four betavoltaic microbatteries: (a) ^{63}Ni–Si, (b) ^{147}Pm–Si, (c) ^{63}Ni–GaAs, and (d) ^{147}Pm–GaAs.

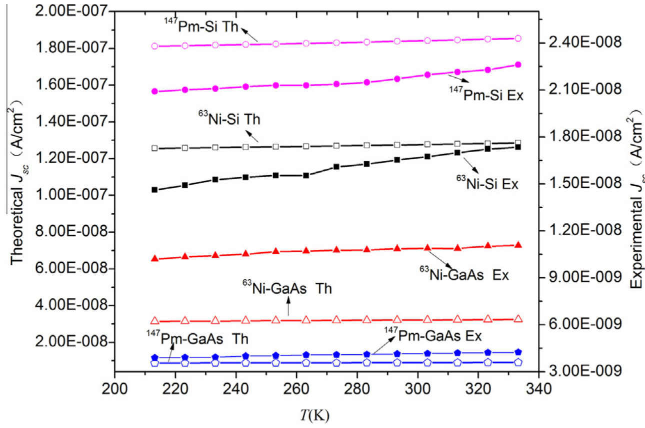

Fig. 5. Experimental and theoretical relationship between J_{SC} and temperature. Ex indicates the experimental value of the J_{SC}, whereas Th indicates the theoretical value.

Table 5
The R of the four kinds of microbatteries.

Betavoltaic microbattery	Range (μm)	
	For the energy of E_{max}	For the energy of E_α
^{63}Ni–Si	27.98	3.07
^{63}Ni–GaAs	12.13	1.33
^{147}Pm–Si	216.26	25.51
^{147}Pm–GaAs	93.83	11.07

the same. As the temperature increases, the inverse of the slope of the curves in the open point and in the short-circuit density point decrease gradually.

3.2. Short-circuit current density

The experimental value of J_{SC} can be obtained based on the intersection point of the curve and the vertical axis in Fig. 4. The theoretical value of J_{SC} can be obtained using Eq. (1). The experimental and theoretical values are shown in Fig. 5. Both experimental and theoretical values show that the J_{SC} values of the four types of microbatteries slightly increase with temperature. This observation is attributed mainly to the decrease in bandgap of the semiconductor materials with the increase in temperature. The energy required for the formation of electron–hole pair slightly reduces, whereas the radioactive source is affected by temperature, hence the number of electron–hole pairs increases. As temperature rises from 213.15 K to 333.15 K, for Si, E_g drops from 1.1316 eV to 1.1016 eV with a reduction of 2.65%, leading to a decrease in ε by 2.28% and an increase in the number of electron–hole pairs by 2.33%. These changes imply that the number increases by only 0.019%/K. For GaAs, the number increases by only 0.030%/K. Therefore, the increase in the number of electron–hole pairs causes J_{SC} to increase slightly with temperature.

According to the obtained experimental and calculated J_{SC} values, the curves of J_{SC} with regard to T are plotted in Fig. 5. The theoretical values is significantly higher than the experimental value. This observation is a result of the backscattering of the secondary electron, collection efficiency of electron–hole pairs in the theoretical analysis, and influence of the leakage current in testing.

The range of beta particles in semiconductor materials R can be calculated by [20]

$$R = 0.412E^{1.265-0.0954\ln E}/\rho, \tag{6}$$

where E is the energy of beta particles (MeV) and ρ is the density of the material (g/cm^3). The maximum energy (E_{max}) and E_α of ^{63}Ni and ^{147}Pm can be obtained in Table 1, and the ρ of Si and GaAs are 2.33 and 5.37 g/cm^3, respectively. Hence, considering the E_{max} and E_α, the R of the four kinds of microbatteries can be calculated and shown in Table 5.

For ^{147}Pm–Si and ^{63}Ni–Si, the thickness of the intrinsic layer is 300 μm and larger than the R. Hence, all of the beta particles which enter into the intrinsic layer are absorbed. According to Eq. (1), the power density deposited in the intrinsic layer can be calculated by

$$p = E_\alpha A_\alpha (1-\eta_\beta)\exp(-\mu w_{d1})(1-\exp(-\mu w_{d2})) \tag{7}$$

Hence, the p of ^{147}Pm–Si and ^{63}Ni–Si can be calculated and they were 6.647×10^{-7} and 4.608×10^{-7} w/cm^2, and the former is larger. As a result, the J_{SC} of ^{147}Pm–Si is larger than that of ^{63}Ni–Si. It can be found in Fig. 5.

For ^{147}Pm–GaAs and ^{63}Ni–GaAs, the intrinsic layer is only 4 μm leading to a part of the beta particles are absorbed. According to Eq. (7), the p of ^{147}Pm–GaAs and ^{63}Ni–GaAs can be calculated and they are 4.015×10^{-8} and 1.443×10^{-7} w/cm^2 and the former is smaller. Hence, the J_{SC} of ^{147}Pm–GaAs is smaller than that of ^{63}Ni–GaAs as shown in Fig. 5.

As shown in Fig. 5, both the experimental J_{SC} of the ^{63}Ni–Si and ^{63}Ni–GaAs increase slightly with the temperature, however, the growth of the former is larger. The same trend can be observed in the theoretical calculations. This finding can be attributed to two reasons. First, the η_β and w_{d2} of ^{63}Ni–Si and ^{63}Ni–GaAs are different. According to a database [21], η_β is larger because the high atomic number of the material. Compared with GaAs, the w_{d2} of Si was enough thick. Hence, more electrons enter the intrinsic layer of Si. Second, the bandgap of Si is smaller than that of GaAs. As a result, ε of Si is smaller than that of GaAs and more electron–hole pairs generated in Si. Thus, J_{SC} of ^{63}Ni–Si is larger than that of ^{63}Ni–GaAs, in a similar fashion, J_{SC} of ^{147}Pm–Si is larger than that of ^{147}Pm–GaAs.

3.3. Reverse saturation current density

J_0 is also an important factor that affects the output of the betavoltaic microbatteries. J_0 can be expressed as [13]:

$$J_0 = \frac{qn_i(w_n + w_p)}{\sqrt{\tau_n \tau_p}}, \tag{8}$$

where n_i is the intrinsic carrier density that is significantly affected by temperature, w_n and w_p are the n-type and p-type depletion widths, τ_n and τ_p are the electron and hole lifetime, and w_n, w_p, τ_n, and τ_p are slightly affected by temperature. n_i can be expressed as:

$$n_i = \sqrt{N_c N_V}\exp\left(-\frac{E_g}{2kT}\right), \tag{9}$$

where N_C and N_V are the effective densities of the state of the electrons in the conduction band and holes in valence band. For Si, N_C and N_V are equal to 2.6×10^{19} $(T/300)^{3/2}$ and 1.04×10^{19} $(T/300)^{3/2}$, respectively. For GaAs, N_C and N_V are equal to 4.7×10^{17} $(T/300)^{3/2}$ and 7×10^{18} $(T/300)^{3/2}$, respectively [22]. J_0 can be uniformly expressed as:

$$J_0 = M\left(\frac{T}{300}\right)^{3/2}\exp\left(-\frac{E_g}{2kT}\right), \tag{10}$$

where M is a constant related to the material. In Si and GaAs, the curve of the dark current considering V was measured respectively at 300 K, as shown in Fig. 6. According to the computing method of Li [23], the reverse saturation current density of Si and GaAs are 9.76×10^{-10} and 3.48×10^{-10} (A/cm^2), respectively. Thus, according to Eq. (10), for Si and GaAs, M is 2.716 and 294.115, respectively. Eq. (10) can be converted into Eq. (11).

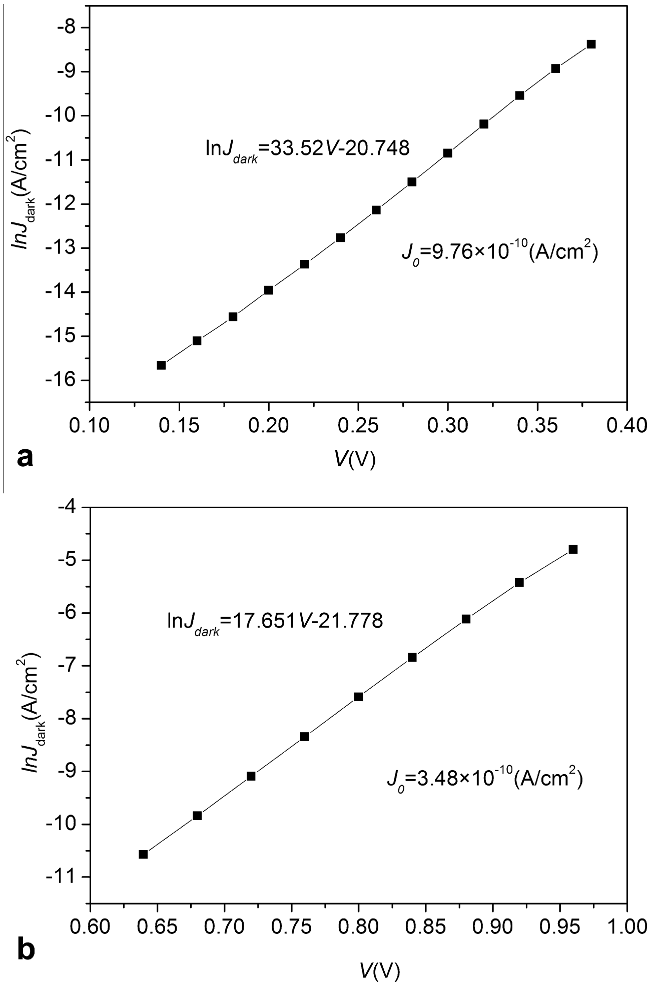

Fig. 6. $\ln J_{\mathrm{dark}}$–V curves of (a) Si, and (b) GaAs.

$$\ln J_0 = \ln M\left(\frac{T}{300}\right)^{3/2} - \frac{E_g}{2kT} \quad (11)$$

From 213.15 K to 333.15 K, $\frac{E_g}{2kT}$ value is much greater than $\ln M(\frac{T}{300})^{3/2}$ value, therefore $\ln J$ and $1/T$ have an approximately liner relationship, as shown in Fig. 7. For Si and GaAs, the difference

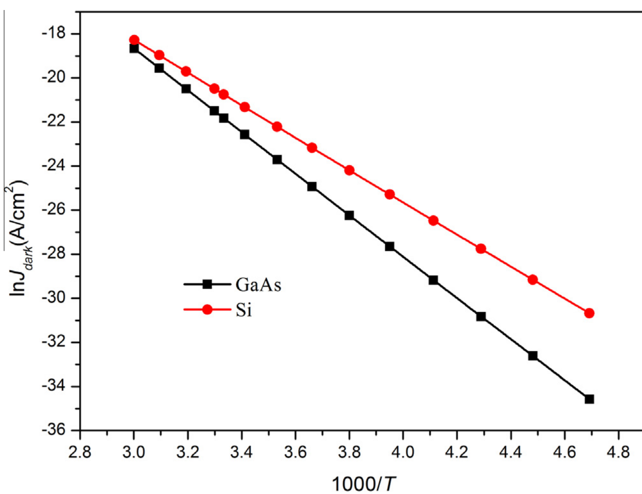

Fig. 7. $\ln J_{\mathrm{dark}}$–V curves of Si and GaAs in the temperature range of 213.15–333.15 K.

shown in Fig. 6 is attributed to the different E_g values, according to Eq. (11). In the same temperature range, $\ln J_0$ of GaAs is smaller than Si and changes more sensitively with increasing temperature because of the larger E_g.

3.4. Open-circuit voltage

By using the values of J_{SC} and J_0, theoretical V_{OC} can be calculated using Eq. (5). By contrast, experimental V_{OC} can be obtained using the intersection point of the curve and the horizontal axis in Fig. 4. The curves of the experimental and theoretical V_{OC} with regard to T are shown in Fig. 7, both values decrease as T rises. The relationship between the theoretical V_{OC} and T is almost linear. In a low temperature, the relationship between experimental V_{OC} and T is almost linear. However, this relationship is not apparent at high temperatures, in which J_{SC} value is much greater than J_0 value, V_{OC} can be approximated by:

$$V_{OC} = \frac{nkT}{q} \ln\left(\frac{J_{SC}}{J_0}\right), \quad (12)$$

where n is the ideal factor. V_{OC} sensitivity can be calculated by

$$\frac{\partial V_{OC}}{\partial T} = \frac{nk}{q} \ln\frac{J_{SC}}{J_0} + \frac{nkT}{qJ_{sc}}\frac{\partial J_{sc}}{\partial T} - \frac{nkT}{qJ_0}\frac{\partial J_0}{\partial T} \quad (13)$$

According to Eq. (10), $\frac{\partial J_0}{\partial T}$ can be obtained using:

$$\frac{\partial J_0}{\partial T} = \frac{J_0}{T}\left(\frac{3}{2} - \frac{1}{2k}\frac{\partial E_g}{\partial T} + \frac{E_g}{2kT}\right) \quad (14)$$

According to the above analysis, the J_{SC} changes slightly with temperature, hence Eq. (13) can be simplified as

$$\frac{\partial V_{OC}}{\partial T} = \frac{nk}{q} \ln\frac{J_{SC}}{J_0} - \frac{n3k}{2q} - \frac{nE_g}{2Tq} - \frac{n\alpha}{2q}\frac{T(T+2\beta)}{(T+\beta)^2} \quad (15)$$

Therefore, V_{OC} sensitivity is negative and decided by J_{SC}, J_0, E_g, α, and β. Table 6 shows the sensitivity of the experimental and theoretical V_{OC} in the linear interval which can be obtained from Fig. 8.

For ^{147}Pm–Si and ^{63}Ni–Si, the intrinsic layer is 300 μm and all of the beta particles which entered into the intrinsic layer are absorbed. Because of the larger J_{SC}, the first item on the right side of Eq. (15) of ^{147}Pm–Si is larger than that of ^{63}Ni–Si. The other items in Eq. (15) were the same. Ultimately, V_{OC} sensitivity of ^{147}Pm–Si was smaller than that of ^{63}Ni–Si.

For ^{147}Pm–GaAs and ^{63}Ni–GaAs, the intrinsic layer is only 4 μm leading to a part of the beta particles are absorbed. According to the values of p, the larger J_{SC} is obtained in ^{63}Ni–GaAs. Hence, the theoretical V_{OC} sensitivity of ^{147}Pm–GaAs is larger than that of ^{63}Ni–GaAs. However, for the experimental V_{OC} sensitivity, the V_{OC} sensitivity of ^{147}Pm–GaAs is smaller than that of ^{63}Ni–GaAs in low temperature (from 213.15 K to 263.15 K). There are inflection points in both the experimental curves of ^{147}Pm–GaAs and ^{63}Ni–GaAs at 263.15 K. However, in high temperature (from 263.15 K to 313.15 K), the V_{OC} sensitivity of ^{147}Pm–GaAs is larger than ^{63}Ni–GaAs and they are −2.39 and −2.22 mV/K, respectively. It may be the actual dopant which is mixed with impurities in the intrinsic layer leading to the appearance of the inflection point.

Table 6
Sensitivities of the theoretical and experimental V_{OC} in the linear interval.

Betavoltaic microbattery	Theoretical (mV/K)	Experimental (linear interval) (mV/K)
^{63}Ni–Si	−1.67	−2.57 (213.15–293.15 K)
^{63}Ni–GaAs	−4.55	−5.30 (213.15–263.15 K)
^{147}Pm–Si	−1.64	−2.53 (213.15–303.15 K)
^{147}Pm–GaAs	−4.65	−4.90 (213.15–263.15 K)

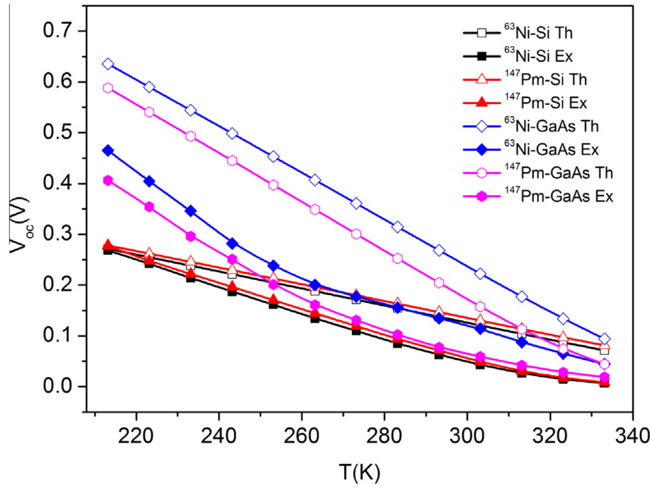

Fig. 8. Curve of theoretical and experimental V_{OC} in terms of T.

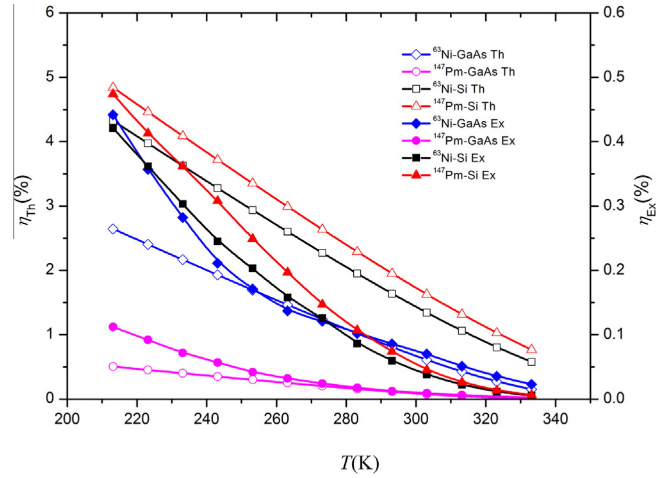

Fig. 9. Experimental and theoretical relationship between η and temperature.

The reason for the inflection point would be researched in the latter work.

When irradiated by the same radioactive sources, V_{OC} sensitivities of the microbatteries are primarily decided by the first item and the last two items of Eq. (15). For GaAs, the value of E_g and n are larger than Si. The absolute value of the V_{OC} sensitivities of the microbatteries based on GaAs is larger. Therefore, the absolute value of the V_{OC} sensitivity of ^{147}Pm–GaAs and ^{63}Ni–GaAs is larger than that of ^{147}Pm–Si and ^{63}Ni–Si, respectively, and the same trend is observed in the experiment, as shown in Table 6.

As shown in Table 6, the V_{OC} sensitivity of the theoretical calculation and experimental measurement differs. According to Eq. (8), V_{OC} sensitivity is related to the ideality factor (n), in theoretical calculation, for Si and GaAs, n are 1 and 2, respectively. In reality, however, at 300 K, the computed n is 1.15 and 2.19 by using the measured dark current curve, according to Li's work [23]. These values are larger than the ideal values that are used in the theoretical calculation. In other temperatures, similar observations are found. Meanwhile, J_0 is based on the J_0 at 300 K, which is calculated using the measured dark current curve that is influenced by the shunt resistance. Thus, a larger theoretical J_0 is obtained. A larger J_0 indicates a lower shunt resistance, which leads to a smaller V_{OC} sensitivity [10]. Hence, a smaller V_{OC} sensitivity is obtained in the calculation.

3.5. Energy conversion efficiency η

The energy conversion efficiency η can be calculated by

$$\eta = \frac{P_{max}}{A_\alpha E_\alpha} \times 100\%, \tag{16}$$

where Pmax is the maximum output power density of the betavoltaic microbatteries. Pmax can be calculated by

$$P_{max} = FF \times J_{SC} \times V_{OC}, \tag{17}$$

where FF is the fill factor and can be calculated by [24]

$$FF = \frac{v_{OC} - \ln(v_{OC} + 0.72)}{v_{OC} + 1}, \tag{18}$$

where v_{OC} is the ratio of V_{OC} and nkT/q. By using the theoretical J_{SC} and V_{OC} as calculated above, the theoretical η can be obtained. According the J–V curves in testing, those parameters can also be obtained and the experimental η can be calculated. For different microbatteries, the theoretical and experimental η are shown in Fig. 9 and the former is one order of magnitude larger than the latter. η is influenced by J_{SC} and V_{OC} which are related to temperature closely. Therefore, as shown in Fig. 9, both theoretical and experimental η decrease evidently with the increase in temperature. The relationship between η and T is almost linear in a low temperature and the linear temperature range is larger for theoretical η. η sensitivity (%/K) can be calculated by

Table 7
Sensitivity of the theoretical and experimental η in the linear interval.

Betavoltaic microbattery	Theoretical (%/K)	Experimental (linear interval) (%/K)
^{63}Ni–Si	−0.733	−1.140 (213.15–283.15 K)
^{63}Ni–GaAs	−0.805	−1.561 (213.15–253.15 K)
^{147}Pm–Si	−0.708	−1.118 (213.15–283.15 K)
^{147}Pm–GaAs	−0.850	−1.607 (213.15–253.15 K)

$$\frac{1}{\eta}\frac{d\eta}{dT} = \frac{1}{\eta}\frac{1}{A_\alpha E_\alpha}\left(\frac{1}{V_{OC}}\frac{dV_{OC}}{dT} + \frac{1}{J_{sc}}\frac{dJ_{sc}}{dT} + \frac{1}{FF}\frac{dFF}{dT}\right), \tag{19}$$

which means the percentage of changes for each degree rise in temperature with respect to the value of η in a certain temperature. According to Fig. 9, the sensitivity of the theoretical and experimental η in the linear interval can be obtained and shown in Table 7.

Based on Eq. (19), the η sensitivity is affected by V_{OC}. As shown above, V_{OC} is affected by J_0. However, in this paper, large J_0 is obtained using the measured dark current curve that is influenced by the shunt resistance. The ideal J_0 can be calculated by [25]

$$J_0 = 1.5 \times 10^8 \exp\left(-\frac{E_g}{kT}\right) \tag{20}$$

which is much smaller than the measured J_0 used in the calculation above. After calculating the two kinds of J_0, it can be found that the difference of the J_0 for GaAs is larger than that for Si. Furthermore, the V_{OC} is affected. As a result, the η sensitivities of GaAs based microbatteries are larger than that of Si based microbatteries. Considering the ideal J_0, for example, the η sensitivity of ^{63}Ni–GaAs and ^{63}Ni–Si are −0.500 and −0.721%/K, respectively. Hence, based on the ideal J_0, the η sensitivities of GaAs based microbatteries are smaller than that of Si based microbatteries.

4. Conclusion

The effects of temperature on four types of betavoltaic microbatteries, namely, ^{63}Ni–Si, ^{147}Pm–Si, ^{63}Ni–GaAs, and ^{147}Pm–GaAs were investigated. By using a simplified theoretical calculation,

the relationship between J_{SC} and T was obtained and found to be consistent with the experimental measurement. The J_{SC} values of ^{63}Ni–GaAs and ^{147}Pm–GaAs were smaller than that of ^{63}Ni–Si and ^{147}Pm–Si. The J_0 values of the betavoltaic microbatteries based on GaAs were smaller than that of the betavoltaic microbatteries based on Si. In addition, the J_0 value easily changes with the increase in temperature. For microbatteries based on Si, the V_{OC} sensitivity of ^{147}Pm–Si was smaller than that of ^{63}Ni–Si. For microbatteries based on GaAs, the theoretical V_{OC} sensitivity of ^{147}Pm–GaAs was larger than that of ^{63}Ni–GaAs; the experimental V_{OC} sensitivity of ^{147}Pm–GaAs is smaller than that of ^{63}Ni–GaAs in low temperature but the experimental V_{OC} sensitivity of ^{147}Pm–GaAs is larger in high temperature.

Moreover, for microbatteries irradiated by the same radioactive source, the V_{OC} sensitivities of the microbatteries based on GaAs were higher than that that of the microbatteries based on Si. η decreased evidently with the increase in temperature. Because of the large J_0, the η sensitivities of GaAs based microbatteries were larger than that of Si based microbatteries. Therefore, higher V_{OC} can be obtained by choosing a semiconductor material with larger bandgap for the for the energy conversion device; however, V_{OC} sensitivity will also be high. The different effects of temperature on the characteristic parameters should be considered to guarantee normal working performance of devices when materials with larger bandgaps are used in betavoltaic microbatteries manufactured in places where temperature changes dynamically.

Acknowledgments

This work was supported by the National Natural Science Foundation of China (Grant No. 11205088), the Natural Science Foundation of Jiangsu Province (Grant No. BK20141406), and the Priority Academic Program Development of Jiangsu Higher Education Institutions.

Appendix A. Supplementary material

Supplementary data associated with this article can be found, in the online version, at http://dx.doi.org/10.1016/j.nimb.2015.07.046.

References

[1] H.M. Chen, Study on Betavoltaic Microbatteries, National Tsing Hua University, Taiwan, 2003.
[2] J. Blanchard, D. Henderson, A. Lal. A Nuclear Microbattery for MEMS Devices. US Deportment of Energy Award No. DEFG07-99ID13781. University of Wisconsin-Madison. Madison, WI, 2002, pp. 53706-10–53706-10.
[3] T.J. Shen, D.H. Liang, J.H. Cai, Z.M. Dai, H.H. Xia, J.H. Wang, L. Sun, G.J. Yu, X. Wang, D.X. Wang, X. Liu, Radioactive isotope battery with unique use, Nucl. Tech. 33 (8) (2010) 625–630.
[4] L. Hong, X.B. Tang, Z. H Xu, Y.P. Liu, D. Chen, Radioluminescent nuclear batteries with different phosphor layers, Nucl. Instrum. Meth. B 338 (2014) 112–118, http://dx.doi.org/10.1016/j.nimb.2014.08.005.
[5] M.A. Prelas, C.L. Weaver, M.L. Watermann, E.D. Lukosi, R.J. Schott, D.A. Wisniewski, A review of nuclear batteries, Prog. Nucl. Energy 75 (2014) 117–148, http://dx.doi.org/10.1016/j.pnucene.2014.04.007.
[6] H. Li, A. Lal, J. Blanchard, D. Henderson, Self-reciprocating radioisotope-powered cantilever, J. Appl. Phys. 92 (2) (2002) 1122–1127, http://dx.doi.org/10.1063/1.1479755.
[7] G.Q. Wang, R. Hu, H.Y. Wei, H.M. Zhang, Y.Q. Yang, X.L. Xiong, G.P. Liu, S.Z. Luo, The effect of temperature changes on electrical performance of the betavoltaic cell, Appl. Radiat. Isotopes 68 (2010) 2214–2217, http://dx.doi.org/10.1016/j.apradiso.2010.06.011.
[8] Y.P. Liu, X.B. Tang, Z. H Xu, L. Hong, P. Wang, D. Chen, Optimization and temperature effects on sandwich betavoltaic microbattery, Sci. China Technol. Sci. 57 (1) (2014) 14–18, http://dx.doi.org/10.1007/s11431-013-5413-0.
[9] G.R.G. Nejad, F. Rahmani, G.R. Abaeiani, Design and optimization of beta-cell temperature sensor based on ^{63}Ni–Si, Appl. Radiat. Isotopes 86 (2014) 46–51, http://dx.doi.org/10.1016/j.apradiso.2013.12.027.
[10] M.V.S. Chandrashekhar, R. Duggirala, G.M. Spencer, A. Lal, 4H SiC betavoltaic powered temperature transducer, Appl. Phys. Lett. 91 (5) (2007) 053511-1–053511-3. Doi:10.1063/1.2767780.
[11] Y.P. Liu, X.B. Tang, Z.H. Xu, L. Hong, H. Wang, M. Liu, D. Chen, Influences of planar source thickness on betavoltaics with different semiconductors, J. Radioanal. Nucl. Chem. 304 (2) (2015) 517–525, http://dx.doi.org/10.1007/s10967-014-3879-2.
[12] T. Wacharasindhu, B.R. Nullmeyer, J.W. Kwon, J.D. Robertson, A.Y. Garnov, Mechanisms leading to losses in conventional betavoltaics and evolution: utilizing composite semiconductor with infused radioisotope for efficiency improvement, J. Microelectromech. Syst. 23 (1) (2014) 56–65, http://dx.doi.org/10.1109/JMEMS.2013.2288523.
[13] X.B. Tang, L. Hong, Z.H. Xu, Y.P. Liu, D. Chen, Temperature effect of a radioluminescent nuclear battery based on 147Pm/ZnS:Cu/GaAs, Appl. Radiat. Isot. 97 (2015) 118–124.
[14] K.E. Bower, Y.A. Barbanel, Y.G. Shreter, G.W. Bohnert, Polymers, Phosphors, and Voltaics for Radioisotope Microbatteries, CRC Press, Florida, 2002.
[15] C.A. Klein, Bandgap dependence and related features of radiation ionization energies in semiconductors, J. Appl. Phys. 39 (4) (1968) 2029–2038.
[16] S.S. Li, Semiconductor Physical Electronics, Plenum Press, New York, 1993.
[17] H.W. Thummel, Durchgang von elektronen und betastrahlung durch materieschichten, akademie-verlag, Berlin, 1974.
[18] ICRP, Radionuclide Transformations-energy and Intensity of Emissions. ICRP Publication 38. Ann. ICRP 11–13, 1983.
[19] H. Drescher, L. Reimer, H. Seidel, Backscattering and secondary electron emission of 10–100 keV electrons in scanning electron microscopy, Z. Angew. Physik 29 (6) (1970) 331–336.
[20] L. Katz, A.S. Penfold, Range-energy relations for electrons and the determination of beta-ray end-point energies by absorption, Rev. Mod. Phys. 24 (1) (1952) 28–44.
[21] D.C. Joy, A database on electron-solid interactions, Scanning 17 (5) (1995) 270–275.
[22] X.L. Ye, Semiconductor Physics, Higher Education Press, Beijing, 2007.
[23] X.Y. Li, Y. Ren, X.J. Chen, D.Y. Qiao, W.Z. Yuan, 63Ni schottky barrier nuclear battery of 4H-SiC, J. Radioanal. Nucl. Chem. 287 (1) (2011) 173–176, http://dx.doi.org/10.1007/s10967-010-0746-7.
[24] X.B. Tang, Y.P. Liu, D. Ding, D. Chen, Optimization design of GaN betavoltaic microbattery, Sci. China Technol. Sci. 55 (3) (2012) 659–664, http://dx.doi.org/10.1007/s11431-011-4739-8.
[25] M.A. Green, Solar Cells: Operating Principles, Technology, and System Applications, Prentice Hall, Englewood Cliffs, NJ, 1982.